Tumor Dose Response to the Vascular Disrupting Agent, 5,6-Dimethylxanthenone-4-Acetic Acid, Using *In vivo* Magnetic Resonance Spectroscopy

Lesley D. McPhail,[1] Yuen-Li Chung,[1] Basetti Madhu,[1] Simon Clark,[2] John R. Griffiths,[1] Lloyd R. Kelland,[2] and Simon P. Robinson[1]

Abstract

Purpose: To use ^{31}P and ^{1}H magnetic resonance spectroscopy (MRS) to assess changes in tumor metabolic profile *in vivo* in response to 5,6-dimethylxanthenone-4-acetic acid (DMXAA) with a view to identifying biomarkers associated with tumor dose response.

Experimental Design: *In vivo* ^{31}P and ^{1}H MRS measurements of (*a*) tumor bioenergetics [β-nucleoside triphosphate/inorganic phosphate (β-NTP/Pi)], (*b*) the membrane-associated phosphodiesters and phosphomonoesters (PDE/PME), (*c*) choline (mmol/L), and (*d*) lactate/water ratio were made on murine HT29 colon carcinoma xenografts pretreatment and 6 or 24 hours posttreatment with increasing doses of DMXAA. Following *in vivo* MRS, the tumors were excised and used for high-resolution ^{31}P and ^{1}H MRS of extracts to provide validation of the *in vivo* MRS data, histologic analysis of necrosis, and high-performance liquid chromatography.

Results: Both β-NTP/Pi and PDE/PME decreased in a dose-dependent manner 6 hours posttreatment with DMXAA, with significant decreases in β-NTP/Pi with 15 mg/kg ($P < 0.001$) and 21 mg/kg ($P < 0.01$). A significant decrease in total choline *in vivo* was found 24 hours posttreatment with 21 mg/kg DMXAA ($P < 0.05$); this was associated with a significant reduction in the concentration of the membrane degradation products glycerophosphoethanolamine and glycerophosphocholine measured in tissue extracts ($P < 0.05$).

Conclusions: The reduction in tumor energetics and membrane turnover is consistent with the vascular-disrupting activity of DMXAA. ^{31}P MRS revealed tumor response to DMXAA at doses below the maximum tolerated dose for mice. Both ^{31}P and ^{1}H MRS provide biomarkers of tumor response to DMXAA that could be used in clinical trials.

Blood flow is essential for the delivery of oxygen and vital nutrients to a growing tumor and for the subsequent removal of cellular waste products. Therefore, the development of a functional vascular network, a process known as angiogenesis, is a prerequisite for tumors to grow beyond 1 to 2 mm in size (1). The tumor vascular network has many differing features in its architecture compared with the vascular network of normal tissues (2). For example, the structure is highly disorganized and blood vessels themselves are dilated and leaky due to the presence of a discontinuous membrane, a characteristic that causes high interstitial fluid pressure (3, 4). Physiologic conditions of the tumor microenvironment (e.g., overexpression of proangiogenic growth factors, hypoxia, and acidosis) cause the proliferation rate of tumor blood vessel endothelium to be 35-fold faster than that of the quiescent endothelium of normal vessels (5). Nevertheless, the cell density of a growing tumor increases at a more rapid rate than its vascular network can support. As a result, each blood vessel often supports a large mass of tumor cells; thus, the destruction of one blood vessel can lead to extensive tumor cell death (6).

Because of its importance in tumor growth and survival, the tumor vascular network has become an attractive target for cancer therapy. Vascular disrupting agents are a class of novel cancer therapeutics that exploit the unstable, immature characteristics of tumor blood vessels to selectively target and destroy the tumor vascular network (7, 8). Vascular disrupting agents can be divided into two categories: ligand-based therapy and small-molecule drugs (8). There are two main classes of small-molecule drugs, the tubulin depolymerizing agents and the flavonoids (or cytokine inducers). 5,6-Dimethylxanthenone-4-acetic acid (DMXAA) is a cytokine-inducing, small molecule vascular-disrupting agent that has recently completed phase 1 clinical trials (9, 10). DMXAA was originally synthesized as a more potent analogue of flavone acetic acid (9), as, despite showing excellent preclinical activity, flavone acetic acid was

Authors' Affiliations: [1]Department of Basic Medical Sciences, St. George's Hospital Medical School and [2]Antisoma Research, Ltd., London, United Kingdom
Received 12/7/04; revised 2/9/05; accepted 2/24/05.

Grant support: Antisoma Research, Ltd., Cancer Research UK, and The Royal Society.

The costs of publication of this article were defrayed in part by the payment of page charges. This article must therefore be hereby marked *advertisement* in accordance with 18 U.S.C. Section 1734 solely to indicate this fact.

Note: S.P. Robinson is the recipient of a Royal Society University Research Fellowship.

Requests for reprints: Lesley McPhail, Department of Basic Medical Sciences, St. Georges Hospital Medical School, Cranmer Terrace, Tooting, SW17 ORE London, United Kingdom. Phone: 44-208-725-5809; Fax: 44-208-725-2992; E-mail: lesley@sghms.ac.uk.

unable to exert the same effect in human tumors (10). The antitumor action of DXMAA involves both direct effects, in the form of endothelial cell apoptosis (11), and indirect effects, through the induction of cytokines *in situ* within the tumor microenvironment (12, 13). The primary cytokine induced by DMXAA is tumor necrosis factor-α, which is known to cause vascular collapse and hemorrhage of tumor blood vessels (14). Overall, the cascade of antivascular effects brought about by DMXAA causes the occlusion and collapse of tumor blood vessels that culminates in the onset of hemorrhagic necrosis and tumor cell death due to prolonged ischemia.

DMXAA and other vascular-disrupting agents are classed as cytostatic drugs as there is often no visible tumor shrinkage in response to treatment, but tumor growth after treatment may be delayed. The cytostatic response induced by vascular-disrupting agents typically causes large central necrosis but leaves a viable rim of cells at the periphery of the tumor that eventually causes tumor cell repopulation (7). Due to the nature of its antitumor action, the clinical development of DMXAA requires biomarkers that will show any response to the drug. Thus far, dynamic contrast–enhanced magnetic resonance imaging has been the method of choice in clinical trials. Dynamic contrast–enhanced magnetic resonance imaging was used in phase 1 clinical trials to evaluate tumor blood flow in response to DMXAA (500-4,900 mg/m^2; refs. 15–17). Although a reduction in tumor blood flow was seen across a wide spectrum of doses, the study failed to establish tumor dose response to DMXAA.

In vivo magnetic resonance spectroscopy (MRS) is a noninvasive method for the assessment of tumor biochemistry and physiology in response to therapy. ^{31}P MRS provides information on tumor energetics; changes in ^{31}P MRS parameters may be linked to changes in tumor perfusion (18, 19). ^{1}H MRS provides information on tumor phospholipids associated with cell membrane turnover, and changes in ^{1}H MRS parameters may be indicative of cell proliferation status (20, 21). In the present study, both *in vivo* ^{31}P and ^{1}H MRS were used to identify early changes in the energetics and membrane turnover of a human colon cancer xenograft with response to increasing doses of DMXAA in an attempt to find a method that would indicate tumor dose response. Both ^{1}H and ^{31}P MRS can be used to monitor the biochemistry of tumors in patients, so it was also of interest to see whether responses to DMXAA measured by these methods might be applicable in clinical trials of the drug. High-resolution MRS of tumor extracts was also used for validation of *in vivo* MRS data and to provide even greater sensitivity to further investigate the biochemical alterations that occur in tumors in response to DMXAA especially at the level of phospholipid metabolism.

Materials and Methods

Tumor cell line. The HT29 human colon carcinoma cell line was maintained in McCoys 5A medium (Life Technologies, Grand Island, NY), supplemented with 10% fetal bovine serum (Life Technologies) and 1% penicillin-streptomycin (Life Technologies). The cells were incubated at 37°C in a 175 mL tissue culture flask in a humidified atmosphere of 5% CO_2 and 95% air. When the cells became confluent, they were harvested using trypsin-EDTA (Life Technologies) and suspended in supplemented medium before injection into mice.

Animals and tumors. Animals were treated in accordance with local and national ethical requirements and with the United Kingdom Coordinating Committee on Cancer Research Guidelines for the Welfare of Animals in Experimental Neoplasia (22). Male MF1 nude mice, 6 to 8 weeks old, were anesthetized using halothane and 5×10^6 cells were injected s.c. into the right flank of each mouse using a 25-gauge needle. Tumor weight was measured using calipers assuming an ellipsoid shape and the formula $l \times w \times d \cdot (\pi / 6)$. Tumors were subsequently used for MRS when they reached a volume of ~700 mg (typically ~1 month after cells were injected).

Administration of 5,6-dimethylxanthenone-4-acetic acid. DMXAA was dissolved in sterile water and administered to mice by a single i.p. injection. Magnetic resonance spectra were acquired from HT29 tumors pretreatment and either 6 or 24 hours after administration of 0, 7.5, 15, or 21 mg/kg DMXAA.

Assessment of tumor bioenergetics by* in vivo *^{31}P magnetic resonance spectroscopy. Anesthesia was induced with an i.p. injection (10 mg/mL) of a combination of fentanyl citrate (0.315 mg/mL) plus fluanisone (10 mg/mL; Hypnorm, Janssen Pharmaceutical, Oxford, United Kingdom) and midazolam (5 mg/mL; Hyponovel, Roche, Welwyn Garden City, Herts, United Kingdom). The mouse was positioned on a platform so that the tumor hung down into a 12 mm, two-turn dedicated ^{31}P surface coil. A plastic water blanket with warm circulating water was used to keep the mouse core temperature at 37°C. ^{31}P MRS was done in a 30 cm horizontal bore, 4.7-T superconducting magnet (Oxford Instruments, Abingdon, Oxfordshire, United Kingdom) at a resonance frequency of 81 MHz. Data acquisition and processing were carried out on a Varian spectrometer (Varian NMR Instruments, Palo Alto, CA). Field homogeneity was optimized by shimming on the tumor to a linewidth typically of 30 to 60 Hz. Tumor scout ^{1}H images were acquired to identify a 9 mm cubic voxel that excluded nontumor tissue. Subsequently, localized ^{31}P spectra were acquired from this voxel using the image-selected *in vivo* spectroscopy pulse sequence (23) with a repetition time of 3 seconds and a total acquisition time of 30 minutes. Spectral analysis was done using MRUI software (24, 25). Signals were assigned as phosphomonoesters (PME), inorganic phosphate (Pi), phosphodiesters (PDE), phosphocreatine, and the three nucleoside triphosphates (α-NTP, β-NTP, and γ-NTP; ref. 26). From the peak areas, β-NTP/Pi, Pi/ΣP, PDE/ΣP, PME/ΣP, and PME/PDE ratios were then determined, where ΣP is the sum of all measured amplitudes.

Assessment of tumor choline concentration and lactate by* in vivo *^{1}H magnetic resonance spectroscopy. Immediately following ^{31}P MRS, the mouse was set up in the magnet as before with the tumor positioned in a 15 mm, two-turn dedicated ^{1}H surface coil for ^{1}H MRS at a resonance frequency of 200 MHz. Tumor scout ^{1}H images were acquired to identify a 9 mm cubic voxel that excluded nontumor tissue. Field homogeneity was optimized by localized shimming on the tumor to a linewidth typically of 20 Hz. Subsequently, localized ^{1}H spectra were acquired from this voxel using five echo times (*TE* = 20, 68, 136, 272, and 408 milliseconds) and the PRESS localization method with water suppression, a repetition time of 2 seconds, and a total acquisition time of 2 minutes (27). A resonance at 3.2 ppm was identified from total choline. An unsuppressed water spectrum was also acquired with the same acquisition parameters as above. A Multiple Quantum Coherence–edited sequence with outer volume saturated localization, a repetition time of 3 seconds, and a total acquisition time of 3 minutes was used to detect the lactate signal at 1.3 ppm (27). The tumor choline concentration (mmol/L) and lactate/water ratio were subsequently determined using MRUI as previously described. Upon completion of *in vivo* MRS, mice were sacrificed and the tumor, heart, liver, and kidneys were excised. After excision, the tumor was dissected into thirds for high-performance liquid chromatography (HPLC), high-resolution MRS, and histologic analysis of necrosis. All tissues were subsequently frozen in liquid nitrogen as quickly as possible, with exemption of the tumor histology tissue that was fixed in formal saline.

High-resolution ^{31}P and ^{1}H magnetic resonance spectroscopy of tumor extracts. One third of each excised tumor was homogenized and

extracted in 6% perchloric acid. The tissue-acid mixture was then centrifuged and the pH of the supernatant adjusted to 7 using perchloric acid or potassium hydroxide. Following neutralization, extracts were frozen, freeze dried, and reconstituted in 1 mL deuterated water; 0.5 mL of each extract was then transferred to a 5 mm nuclear magnetic resonance tube. *In vitro* ^{1}H and ^{31}P MRS of the tumor extracts were done on a Bruker 600 MHz nuclear magnetic resonance system (Bruker Biospin, Coventry, United Kingdom). For ^{1}H chemical shift calibration and quantitation, sodium 3-trimethylsilyl-2,2,3,3-tetra-deuteropropionate (50 μL, 5 mmol/L) was added to each sample tube. The pH was adjusted to 7 before analysis using perchloric acid or potassium hydroxide. For ^{1}H MRS, the water resonance was suppressed using gated irradiation centered on the water frequency. Metabolite concentrations of lactate, free choline, phosphocholine, and glycerophosphocholine were assigned and quantified from the spectra. After ^{1}H MRS, ^{31}P MRS was done. EDTA (50 μL, 60 mmol/L) was added to each sample for chelation of metal ions and methylene diphosphonic acid (50 μL, 5 mmol/L) was added to samples for ^{31}P chemical shift calibration and quantitation. The pH was again adjusted to 7 before analysis using perchloric acid or potassium hydroxide. The peaks of phosphoethanolamine, phosphocholine, Pi, glycerophosphoethanolamine, and glycerophosphocholine were assigned and quantified from the spectra (26).

Quantitation of 5,6-dimethylxanthenone-4-acetic acid in mouse tissue homogenates using high-performance liquid chromatography. HPLC analyses were done using a HPLC autosampler, a HPLC pump, a UV detector DAD (all from Agilent Technologies, South Queensferry, West Lothian, United Kingdom) and a LUNA LC_{18} column (5 μm, 4.6 × 100 mm; Phenomenex, Cheshire, United Kingdom).

A HPLC-UV bioanalytic method was used for the quantitative determination of DMXAA in homogenates of tumor, heart, liver, and kidneys. DMXAA and the internal standard SN-24350 (2,5-dimethylxanthenone-4-acetic acid, kindly donated by Dr. Philip Kestell, Auckland Cancer Society Research Centre, New Zealand) were extracted from 100 μL homogenate using solvent precipitation. Extracts were evaporated to dryness before reconstitution and analysis. Chromatography was done using a LUNA LC_{18} analytic column (Phenomenex) suitable for chiral isomer separation with an isocratic mobile phase containing acetonitrile (BDH, Poole, Dorset, United Kingdom) and 10 mmol/L ammonium acetate at pH 5 (Sigma, Poole, Dorset, United Kingdom). The flow rate was 2 mL/min and the run time was 10 minutes per sample. Detection of DMXAA and internal standard was via UV adsorption at a wavelength of 254 nm using UV diode-array detection. Data collection and analysis (peak area integration and quantification) was done using Chemstation v10 (Agilent Technologies).

Histology. The remaining third of each excised tumor was fixed in formal saline. Paraffin-embedded sections were cut from this part and stained with Ehrlich's H&E for the assessment of necrosis. Histologic sections were subsequently analyzed by using a qualitative scoring system that divided the tumors into the following categories: grade 1, no necrosis; grade 2, patchy necrosis; grade 3, large central necrosis; or grade 4, extensive necrosis.

Results

In vivo localized ^{31}P magnetic resonance spectra obtained from a HT29 tumor pretreatment and 6 hours after DMXAA treatment are shown in Fig. 1A. Resonances were readily identified as γ-NTP, α-NTP, and β-NTP; Pi; phosphocreatine; and the resonances of the phospholipid metabolites PME (primarily consisting of phosphocholine and phosphoethanolamine) and PDE (primarily consisting of glycerophosphocholine and glycerophosphoethanolamine). Treatment with 21 mg/kg DMXAA resulted in a massive increase in Pi, depletion of the high-energy phosphates, and negligible change in PME. Figure 2A-C shows the measurements of PDE/PME, PDE/ΣP, and β-NTP/Pi in individual tumors pretreatment and 6 hours posttreatment with 21 mg/kg DMXAA. PDE/ΣP and β-NTP/Pi generally decreased after treatment with the drug. Data from the *in vivo* ^{31}P MRS of tumors treated with various doses of DMXAA are summarized in Fig. 3A-C. PDE/PME and PDE/ΣP significantly decreased 6 and 24 hours posttreatment with 21 mg/kg DMXAA. There was also a significant reduction in β-NTP/Pi 6 hours posttreatment with 15 and 21 mg/kg DMXAA, which remained significant at 24 hours posttreatment with 21 mg/kg DMXAA.

In vivo localized ^{1}H magnetic resonance spectra obtained from a HT29 tumor pretreatment and 6 hours post DMXAA treatment are shown in Fig. 1B. A resonance from total choline was detected at a chemical shift of 3.2 ppm. Lactate was also detected in the ^{1}H magnetic resonance spectra obtained from the Multiple Quantum Coherence–edited sequence in HT29 tumors pretreatment and 6 hours posttreatment (Fig. 1C). Measurements of lactate/water ratio and choline (mmol/L) in HT29 tumors of individual mice pretreatment and 6 hours posttreatment with 21 mg/kg DMXAA are illustrated in Fig. 2D and E. There was a general increase in lactate and a general decrease in choline after treatment. The dose-dependent changes in lactate/water ratio and choline (mmol/L) in HT29 tumors pretreatment and 6 hours posttreatment with 0, 7.5, 15, or 21 mg/kg DMXAA, and also 24 hours posttreatment with 21 mg/kg DMXAA, are shown in Fig. 3D and E. Total choline concentration decreased 6 hours posttreatment with 21 mg/kg DMXAA and this reduction became significant 24 hours posttreatment with 21 mg/kg DMXAA.

Phosphorus metabolite levels detected using *in vitro* ^{31}P MRS of tumor extracts, 6 hours posttreatment with 0, 7.5, 15, or 21 mg/kg of DMXAA, are shown in Fig. 4A. Inorganic phosphate significantly increased after treatment with 21 mg/kg DMXAA. There was no significant change in phosphocholine and phosphoethanolamine. A significant decrease in glycerophosphoethanolamine after treatment with 21 mg/kg DMXAA and a significant decrease in glycerophosphocholine after treatment with 15 and 21 mg/kg DMXAA were found. PDE, which consists of glycerophosphoethanolamine and glycerophosphocholine, was significantly reduced after treatment with 15 or 21 mg/kg DMXAA.

Figure 4B shows the metabolites detected using *in vitro* ^{1}H MRS of tumor extracts, 6 hours posttreatment with 0, 7.5, 15, or 21 mg/kg DMXAA. There was a significant increase in free choline and a significant decrease in glycerophosphocholine following administration of 21 mg/kg DMXAA.

The concentrations of DMXAA found in homogenates of tumor, liver, kidney, and heart of mice by HPLC, 6 hours posttreatment with 0, 7.5, 15, or 21 mg/kg DMXAA, are shown in Fig. 5. The chromatographic retention times of DMXAA and the internal standard were ~4.2 and 5.2 minutes, respectively. The concentration of DMXAA within each tissue was found to increase with increasing dose of drug administered.

Histologic sections of a control HT29 tumor and a HT29 tumor 6 hours posttreatment with 21 mg/kg DMXAA are shown in Fig. 6. Posttreatment with DMXAA, the tumors presented with a viable rim and large central necrosis. Using the devised grading system, the control tumor section in Fig. 6A was classed as grade 1 (i.e., no necrosis), whereas the 21 mg/kg DMXAA–treated tumor section in Fig. 6B was classed as grade 3 (i.e., large central necrosis).

Discussion

The aim of this study was to identify early changes in tumor energetics and choline concentrations associated with response to DXMAA in HT29 colon carcinomas in mice with a view to establishing tumor dose response. To this end, *in vivo* ^{31}P and ^{1}H MRS were used in the study as a noninvasive method of investigating changes related to perfusion and cell membrane turnover of tumors in response to DMXAA.

In vivo ^{31}P MRS revealed a dramatic decrease in tumor bioenergetics 6 hours posttreatment with either 15 or 21 mg/kg DMXAA. This response was sustained at 24 hours posttreatment with 21 mg/kg DMXAA. The depletion of high-energy metabolites within the tumor after treatment is consistent with vascular shutdown and indicates that DMXAA is starving the tumor of essential nutrients. A similar response was reported by Beauregard et al. (19), who found significant decreases in perfusion and bioenergetics of HT29 tumors 3 and 6 hours posttreatment with 27.5 mg/kg DMXAA. A significant decrease in the energetic status of C3H mammary carcinomas 6 hours posttreatment with 15 mg/kg DMXAA has also been shown (28).

The PME resonance detected by ^{31}P MRS *in vivo* consists of the phospholipid precursors phosphocholine and phosphoethanolamine, which are converted to phosphatidylcholine and phosphatidylethanolamine, major constituents of cell membranes. PME remained detectable and unchanged 6

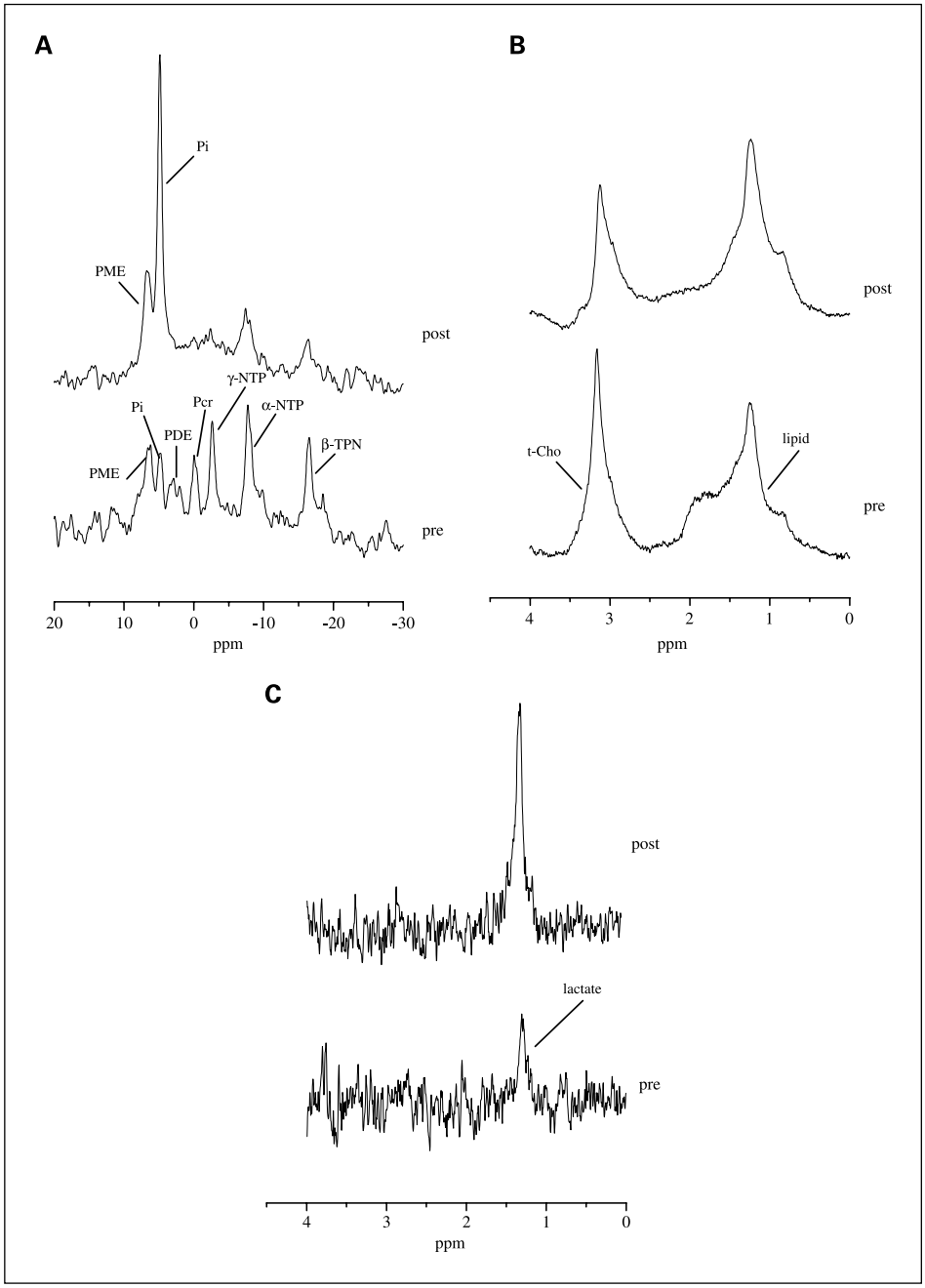

Fig. 1. *A*, localized ^{31}P magnetic resonance spectra of a HT29 tumor pretreatment and 6 hours posttreatment with 21 mg/kg DMXAA. *B*, localized ^{1}H spectra of a HT29 tumor using the PRESS method for choline detection pretreatment and 6 hours posttreatment with 21 mg/kg DMXAA. The resonance at 3.2 ppm is from total choline, whereas the resonance at 1.3 ppm is mainly lipid. *C*, localized ^{1}H spectra of a HT29 tumor using the Multiple Quantum Coherence – edited sequence for lactate detection pretreatment and 6 hours posttreatment with 21 mg/kg DMXAA. The resonance at 1.3 ppm is from lactate.

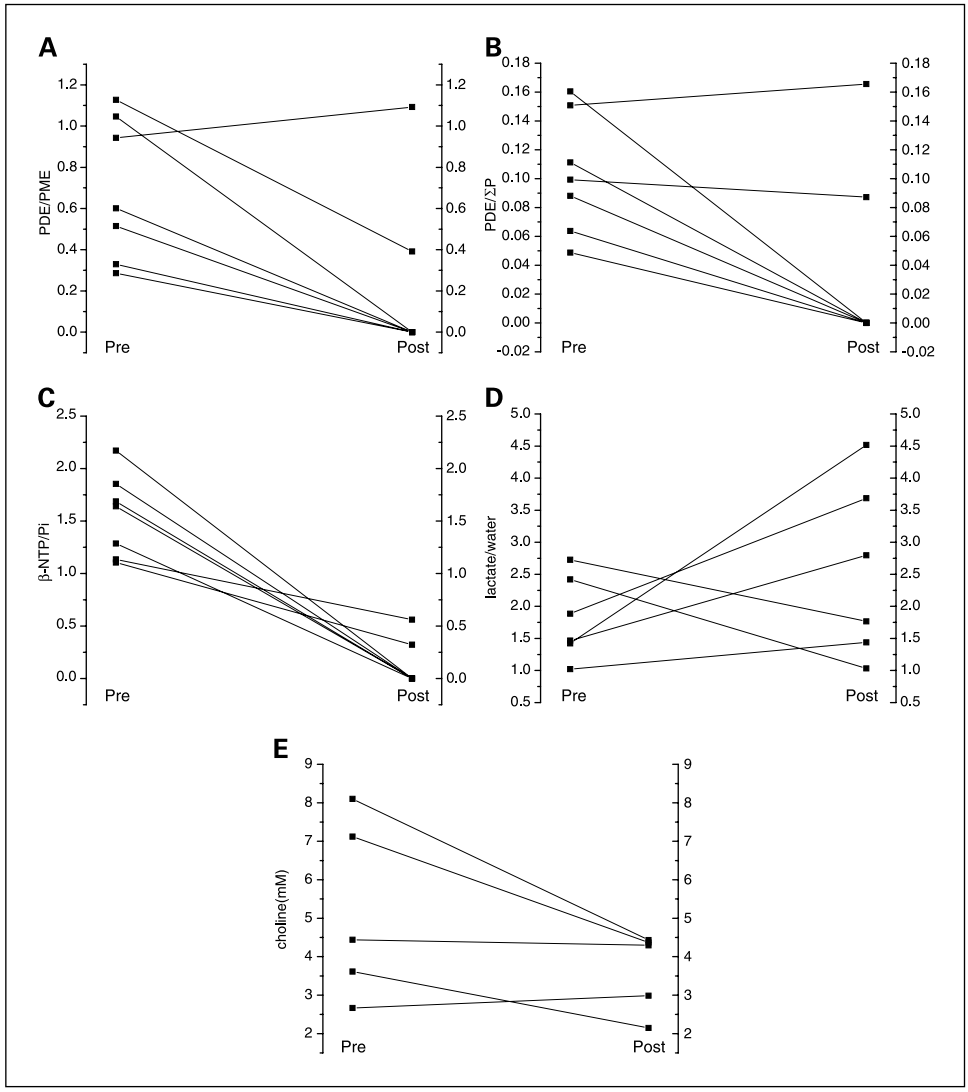

Fig. 2. Line series graphs of PDE/PME (*A*), PDE/ΣP (*B*), β-NTP/Pi (data obtained using *in vivo* ^{31}P MRS; *C*), lactate/water (*D*), and choline (mmol/L; data obtained using *in vivo* ^{1}H MRS; *E*) in individual HT29 tumors pretreatment and 6 hours posttreatment with 21 mg/kg DMXAA.

hours posttreatment with DMXAA. This was confirmed by the high-resolution ^{31}P MRS data, which showed that the concentrations of phosphocholine and phosphoethanolamine remain unchanged after treatment. These results support those obtained by Beauregard et al. (19), who noted that *in vivo* PME was unchanged in the tumor after treatment with DMXAA.

PDE consists of glycerophosphoethanolamine and glycerophosphocholine, which are products of membrane degradation. Unlike PME, PDE was significantly depleted within tumor tissue 6 and 24 hours posttreatment with 21 mg/kg DMXAA.

The choline peak visualized in the *in vivo* ^{1}H spectra is from total choline and consists of phosphocholine, glycerophosphocholine, glycerophosphoethanolamine, phosphoethanolamine, and free choline. Total choline was reduced following treatment with DMXAA. High-resolution ^{31}P and ^{1}H MRS of tissue extracts allow the detection of distinct choline metabolites that contribute to the total choline peak observed *in vivo*. Choline-containing metabolites are associated with cell membrane metabolism; therefore, changes in their concentration detected using *in vivo* ^{31}P and ^{1}H MRS of tumors and *in vitro* ^{31}P and ^{1}H MRS of tumor extracts are indicative of changes in cell membrane turnover. The concentrations of phosphoethanolamine and phosphocholine (membrane precursors) were unchanged after treatment, whereas the concentrations of glycerophosphoethanolamine and glycerophosphocholine (membrane degradation products) were significantly reduced after treatment with 21 mg/kg DMXAA. Furthermore, a significant increase in free choline (i.e., not membrane bound) following treatment with 21 mg/kg DMXAA was found, which suggests that it is no longer being incorporated into cell membranes. These results suggest that DMXAA causes a reduction in cell membrane turnover and proliferation as there is an increase in free choline, which could cause a decrease in membrane precursors (phosphocholine and phosphoethanolamine) and subsequently lead to the observed decrease in membrane degradation products (glycerophosphoethanolamine and glycerophosphocholine). Our results showed that phosphocholine and phosphoethanolamine actually remain unchanged after treatment; this may be due to a decrease in membrane synthesis (hence, increase in free choline) and membrane breakdown (decrease in glycerophosphoethanolamine and glycerophosphocholine levels),

which causes the net levels of phosphocholine and phosphoethanolamine to remain unchanged. Cell proliferation requires energy and, as observed using *in vivo* ^{31}P MRS, there is a reduction of high-energy metabolites within the tumor after treatment with DMXAA. Therefore, the lack of energy within the tumor due to vascular shutdown could lead to a decrease in proliferation and, hence, the observed changes in choline-containing metabolites.

In vivo ^{1}H MRS was also used to investigate changes in lactate. If no oxygen is present and conditions are anaerobic, pyruvate, the end product of glycolysis, is converted to lactate. Although insignificant, there was a trend toward an increase in lactate within tumor tissue 6 hours after treatment with 21 mg/kg DMXAA. The increase in lactate following treatment is consistent with a reduction of oxygen being delivered to the tumor via the blood as a result of vascular shutdown.

DMXAA is extensively metabolized, mainly in the liver, by glucuronidation and 6-methylhydroxylation to give DMXAA acyl glucuronide and 6-hydroxymethyl-5-methylxanthenone-4-acetic acid, respectively (29). HPLC showed that DMXAA remained detectable in tumor tissue 6 hours posttreatment; however, a higher concentration of DMXAA was found in liver and kidney tissues, which is consistent with its route of metabolism and excretion. Preclinical and clinical studies have shown negligible normal tissue toxicity to DMXAA (16, 17, 30, 31).

The accepted mechanism of antitumor action of DMXAA is that it induces vascular collapse and hemorrhage of tumor blood vessels, which in turn leads to necrosis through nutrient and oxygen deprivation within the tumor microenvironment (13). Collectively, the MRS data presented in this study, combined with histologic analysis of tumor necrosis, support the mechanism of action of DMXAA. In our study using mice, a significant dose-dependent reduction in tumor energetics (β-NTP/Pi) using *in vivo* ^{31}P MRS was found after administration of 15 or 21 mg/kg DMXAA. However, regarding cell membrane turnover and proliferation (PDE/PME, PDE/ΣP, and choline concentration), a significant effect was only induced after administration of 21 mg/kg DMXAA (the highest dose used in the study). The maximum tolerated dose of DMXAA in nude mice is 30 mg/kg (32). At the beginning of this study, a 25 mg/kg (75 mg/m^2) dose was also included; however, it proved to be too toxic for the mice and, hence, unethical to continue using. Humans, however, can tolerate much higher doses of DMXAA than

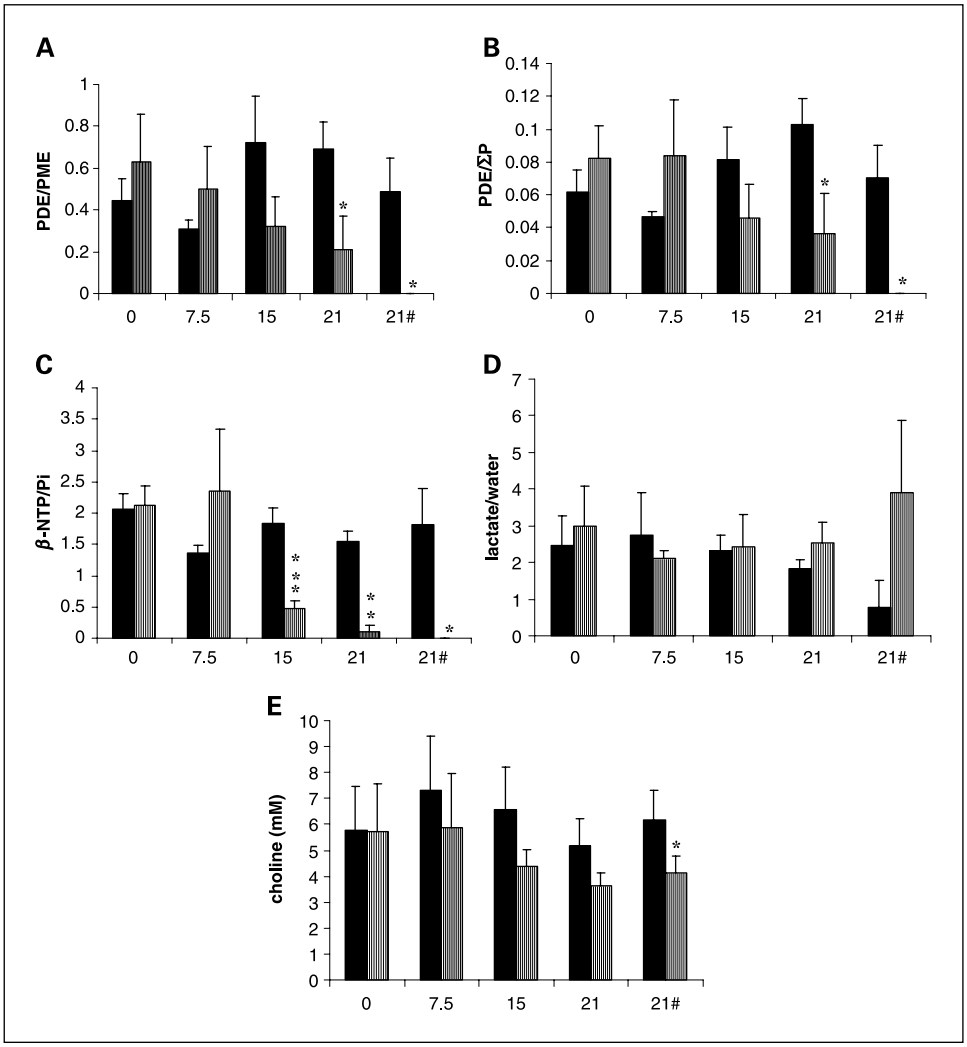

Fig. 3. The use of *in vivo* ^{31}P and ^{1}H MRS to assess tumor dose-response of PDE/PME (control $n = 9$, 7.5 mg/kg $n = 6$, 15 mg/kg $n = 9$, 21 mg/kg $n = 7$, and 21 mg/kg# $n = 5$; *A*), PDE/ΣP (control $n = 9$, 7.5 mg/kg $n = 6$, 15 mg/kg $n = 9$, 21 mg/kg $n = 7$, and 21 mg/kg# $n = 5$; *B*), β-NTP/Pi (control $n = 9$, 7.5 mg/kg $n = 6$, 15 mg/kg $n = 9$, 21 mg/kg $n = 7$, and 21 mg/kg# $n = 5$; *C*), lactate/water (control $n = 6$, 7.5 mg/kg $n = 4$, 15 mg/kg $n = 6$, 21 mg/kg $n = 6$, and 21 mg/kg# $n = 5$; *D*), and choline (mmol/L; control $n = 4$, 7.5 mg/kg $n = 4$, 15 mg/kg $n = 6$, 21 mg/kg $n = 5$, and 21 mg/kg# $n = 5$; *E*) before treatment (*black columns*) and either 6 hours posttreatment (*gray columns*) with 0, 7.5, 15, or 21 mg/kg or 24 hours posttreatment with 21 mg/kg DMXAA (*21#*). Student's paired *t* test, $^{*}P < 0.05$, $^{**}P < 0.01$, and $^{***}P < 0.001$.

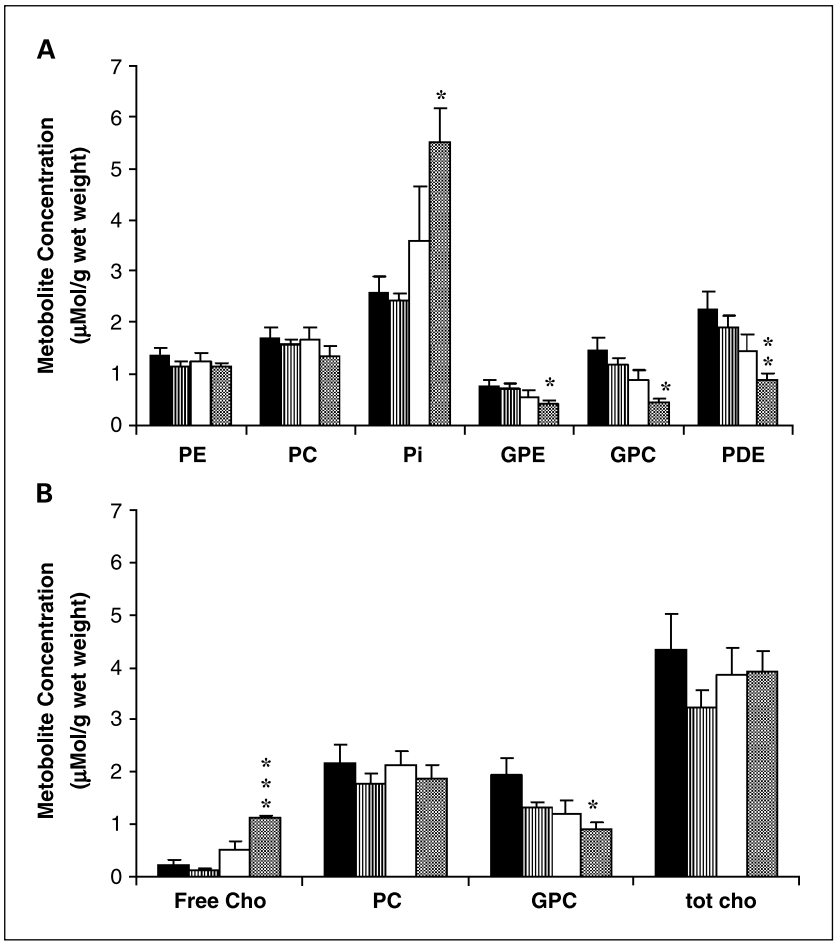

Fig. 4. *A*, phosphorus metabolites detected using high-resolution ^{31}P MRS of tumor extracts 6 hours posttreatment with DMXAA [control (*black columns*) $n = 7$, 7.5 mg/kg (*striped columns*) $n = 6$, 15 mg/kg (*white columns*) $n = 5$, and 21 mg/kg (*hatched columns*) $n = 4$]. Student's paired t test, $^{*}P < 0.05$, $^{**}P < 0.01$, and $^{***}P < 0.001$. *B*, proton metabolites detected using high-resolution ^{1}H MRS of tumor extracts 6 hours posttreatment with DMXAA [control (*black columns*) $n = 7$, 7.5 mg/kg (*striped columns*) $n = 6$, 15 mg/kg (*white columns*) $n = 6$, and 21 mg/kg (*hatched columns*) $n = 4$]. Student's paired t test, $^{*}P < 0.05$, $^{**}P < 0.01$, and $^{***}P < 0.001$.

mice; evidence of blood flow reduction as assessed by dynamic contrast–enhanced magnetic resonance imaging was apparent at doses of 1,100 mg/m^2 with little dose dependency above this level (15).

The responses to DMXAA observed by ^{1}H and ^{31}P MRS in the present study occurred between 50% and 70% of the mouse maximum tolerated dose. Could they have any relevance to trials of the drug in humans in view of the fact that the dynamic contrast–enhanced magnetic resonance imaging responses observed by Galbraith et al. (15) were in the range 10% to 75% of the human maximum tolerated dose? One possible explanation for this difference is that mice are more sensitive than humans to the toxic effects of the drug so the mouse study could not extend over the full dose range used on the patients. The issue of sensitivity makes the use of a mouse model to assess DMXAA questionable. Indeed, it is possible that the maximum response to DMXAA in patients occurred in the lower part of the dose range used by Galbraith et al. and that this was the cause of their failure to detect a dose-response/proportionality. It might, therefore, be appropriate to look for responses with either ^{1}H or ^{31}P MRS during clinical trials of DMXAA. Both these methods can give spectra comparable with those obtained in the present study when used on appropriately sited tumors in patients (33). For example, *in vivo* ^{1}H MRS has recently been successfully used in the clinic to determine total choline concentration of locally advanced breast cancer before and after neoadjuvant chemotherapy to predict response (34).

In conclusion, our results show that both *in vivo* ^{31}P and ^{1}H MRS could be used as noninvasive techniques in the clinic to monitor the response of tumors to DMXAA and other vascular-disrupting agents (19, 28, 35) through changes in tumor energetics and choline concentrations. Our *in vivo* ^{31}P MRS data shows that in mice, there is tumor dose

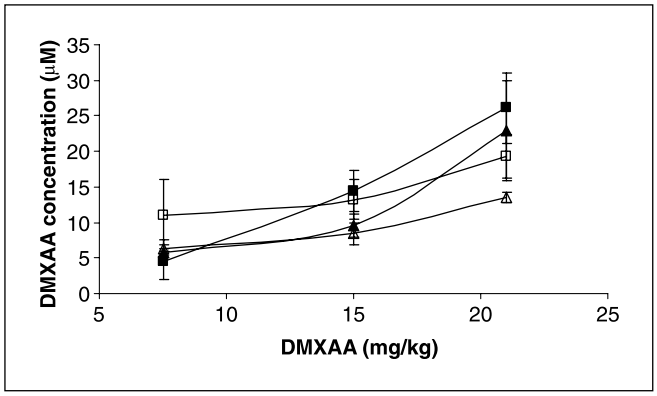

Fig. 5. DMXAA biodistribution in tumor (▲; 7.5 mg/kg $n = 3$, 15 mg/kg $n = 6$, and 21 mg/kg $n = 3$), kidney (□; 7.5 mg/kg $n = 4$, 15 mg/kg $n = 7$, and 21 mg/kg $n = 3$), liver (■; 7.5 mg/kg $n = 4$, 15 mg/kg $n = 7$, and 21 mg/kg $n = 5$), and heart (△; 7.5 mg/kg $n = 3$, 15 mg/kg $n = 5$, and 21 mg/kg $n = 3$) tissue homogenates assessed by HPLC 6 hours posttreatment.

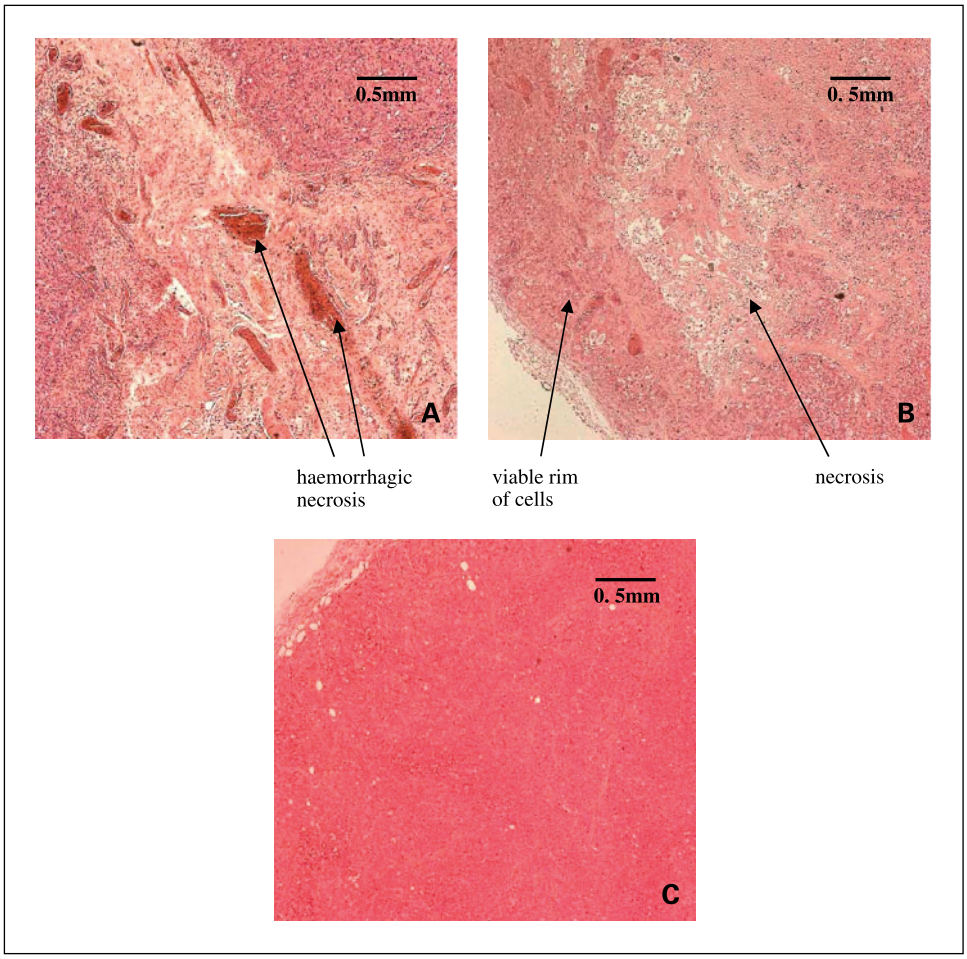

Fig. 6. H&E-stained sections of a HT29 tumor 6 hours posttreatment with 15 mg/kg DMXAA (*A*), a HT29 tumor 6 hours posttreatment with 21 mg/kg DMXAA (*B*), and a control HT29 tumor (*C*).

response to DMXAA with respect to a reduction in energetics (β-NTP/Pi). However, the reduction in cell membrane turnover (PDE/PME, PDE/ΣP, and choline concentrations) seen using *in vivo* ^{1}H MRS is only significant at 21 mg/kg DMXAA, the highest dose used in the study.

Acknowledgments

We thank the Biomics Centre at St. Georges Hospital Medical School for use of the Bruker 600 MHz NMR system and the staff at the Biological Research Facility, St. Georges Hospital Medical School, for supply and maintenance of the animals used.

References

1. Folkman J. How is blood vessel growth regulated in normal and neoplasic tissue?—G.H.A. Clowes memorial award lecture. Cancer Res 1986;46:467–73.
2. Denekamp J. Angiogenesis, neovascular proliferation and vascular pathophysiology as targets for cancer therapy. Br J Radiol 1993;66:181–96.
3. Carmeliet P, Jain RK. Angiogenesis in cancer and other diseases. Nature 2000;407:249–57.
4. Carmeliet P. Angiogenesis in health and disease. Nat Med 2003;9:653–60.
5. Denekamp J, Hobson B. Endothelial-cell proliferation in experimental tumours. Br J Cancer 1982;46:711–20.
6. Chaplin DJ, Dougherty GJ. Tumour vascular as a target for cancer therapy. Br J Cancer 1999;80:57–64.
7. Siemann DW, Chaplin DJ, Horsman MR. Vascular-targeting therapies for treatment of malignant disease. Cancer 2004;100:2491–7.
8. Thorpe PE. Vascular targeting agents as cancer therapeutics. Clin Cancer Res 2004;10:415–27.
9. Rewcastle GW, Atwell GJ, Zhuang L, Baguley BC, Denny WA. Potential antitumour agents. 61. Structure-activity relationships for *in vivo* colon 38 activity among disubstituted 9-oxo-9*H*-xanthene-4-acetic acids. J Med Chem 1991;34:217–22.
10. Kerr DJ, Kaye SB. Flavone acetic acid—preclinical and clinical activity. Eur J Cancer Clin Oncol 1989;25:1271–2.
11. Ching L-M, Cao Z, Kieda C, Zwain S, Jameson MB, Baguley BC. Induction of endothelial cell apoptosis by the anti-vascular agent 5,6-dimethylxanthenone-4acetic acid. B J Cancer 2002;86:1937–42.
12. Joseph WR, Cao Z, Mountjoy KG, Marshall ES, Baguley BC, Ching L-M. Stimulation of tumours to synthesis tumour necrosis factor-α *in situ* using 5,6-dimethylxanthenone-4-acetic acid: a novel approach to cancer therapy. Cancer Res 1999;59:633–8.
13. Baguley BC. Antivascular therapy of cancer: DMXAA. Lancet Oncol 2003;4:141–8.
14. Watanabe N, Niitsu Y, Umeno H, et al. Toxic effect of tumour necrosis factor on tumour vasculature in mice. Cancer Res 1988;48:2179–83.
15. Galbraith SM, Rustin JS, Lodge MA, et al. Effects of 5,6-dimethylxanthenone-4-acetic acid on human tumour microcirculation assessed by dynamic contrast-enhanced magnetic resonance imaging. J Clin Oncol 2002;20:3826–40.
16. Rustin G, Bradley C, Galbraith S, Stratford M. 5,6-Dimethylxanthenone-4-acetic acid (DMXAA), a novel antivascular agent: phase 1 pharmacokinetic and pharmacodynamic study. Br J Cancer 2003;88:1160–7.
17. Jameson MB, Thompson PI, Baguley BC, et al. Clinical aspects of a phase 1 trial of 5,6-dimethylxanthenone-4-acetic acid (DMXAA), a novel antivascular agent. Br J Cancer 2003;88:1844–50.
18. Tozer GM, Bhujwalla ZM, Griffiths JR, Maxwell RJ. Phosphorus-31 magnetic resonance spectroscopy and blood perfusion of the RIF-1 tumour following X-irradiation. Int J Radiat Oncol Biol Phys 1989;16:155–64.
19. Beauregard DA, Pedley RB, Hill SA, Brindle KM. Differential sensitivity of two adenocarcinoma xenografts to the anti-vascular drugs combretastatin A4 phosphate and 5,6-dimethylxanthenone-4-acetic acid, assessed using MRI and MRS. NMR Biomed 2002;15:99–105.
20. Podo F. Tumour phospholipid metabolism. NMR Biomed 1999;12:413–39.
21. Howe FA, Opstad KS. ^{1}H MR spectroscopy of brain tumours and masses. NMR Biomed 2003;16:1–9.
22. United Kingdom Coordinating Committee on Cancer Research. Guidelines for the welfare of animals in experimental neoplasia (2nd ed.). Br J Cancer 1998;77:1–10.
23. Ordidge RJ, Connelly A, Lohman JAB. Image-selected *in vivo* spectroscopy (ISIS). A new technique

for spatially selective NMR spectroscopy. J Magn Reson 1986;66:283–94.

24. Van Der Veen JWC, Beer R DE, Luyten PR, Van Ormondt D. Accurate quantification of *in vivo* ^{31}P NMR signals using the variable projection method and prior knowledge. Magn Reson Med 1988;6:92–8.

25. Van Den Boogaart A, Howe FA, Rodrigues LM, Stubbs M, Griffiths JR. *In vivo* ^{31}P MRS: absolute concentrations, signal-to-noise and prior knowledge. NMR Biomed 1995;8:87–93.

26. Chung Y-L, Troy H, Banerji U, et al. Magnetic resonance spectroscopic pharmacodynamic markers of the heat shock protein 90 inhibitor 17-allylamino, 17-demethoxygeldanamycin (17AAG) in human colon cancer models. J Natl Cancer Inst 2003;95:1624–33.

27. Madhu B, Troy H, Robinson SP, Howe FA, Stubbs M, Griffiths JR. Site dependence of choline concentration in HT29 tumours studied by *in vivo* ^{1}H MR spectroscopy. Proc Intl Soc Magn Reson Med 2003;11.

28. Breidahl T, Nielsen FU, Maxwell RJ, Stoedkilde Joergensen H, Horseman MR. Evaluating the antitumour activity of new vascular damaging agents using magnetic resonance spectroscopy. Proc Intl Soc Mag Reson Med 1999;1333.

29. Kestell P, Paxton JW, Rewcastle GW, Dunlop I, Baguley BC. Plasma disposition, metabolism and excretion of the experimental antitumour agent 5,6-dimethylxanthenone-4-acetic acid in the mouse, rat and rabbit. Cancer Chemother Pharmacol 1999;43:323–30.

30. Murata R, Overgaard J, Horsman MR. Comparative effects of combretastatin A-4 disodium phosphate and 5,6-dimethylxanthenone-4-acetic acid on blood perfusion in a murine tumour and normal tissues. Int J Radiat Biol 2001;77:195–204.

31. Ching L-M, Zwain S, Baguley BC. Relationship between tumour endothelial cell apoptosis and tumour blood flow shutdown following treatment with the antivascular agent DMXAA in mice. Br J Cancer 2004;90:906–10.

32. Zhou S, Kestell P, Baguley BC, Paxton JW. 5,6-Dimethylxanthenone-4-acetic acid (DMXAA): a new biological response modifier for cancer therapy. Invest New Drugs 2002;20:281–5.

33. Griffiths JR, Tate AR, Howe FA, Stubbs M. Magnetic resonance spectroscopy of cancer—practicalities of multi-centre trials and early results in non-Hodgkin's lymphoma. Eur J Cancer 2002;38:2085–93.

34. Meisamy S, Bolan PJ, Baker EH, et al. Neoadjuvant chemotherapy of locally advanced breast cancer: predicting response with *in vivo* ^{1}H MR spectroscopy—a pilot study at 4T. Radiology 2004;233:424–31.

35. Madhu B, Griffiths JR, Ryan AS, Waterton JC, Robinson SP. The response of RIF-1 fibrosarcomas to the vascular targeting drug ZD6126 assessed by *in vivo* ^{1}H-MRS. Proc Intl Soc Mag Reson Med 2004;2033.